Alexander Pimenov; Dmitrii Rachinskii

Homoclinic orbits in a two-patch predator-prey model with Preisach hysteresis operator

HOMOCLINIC ORBITS IN A TWO-PATCH PREDATOR-PREY MODEL WITH PREISACH HYSTERESIS OPERATOR

ALEXANDER PIMENOV, Berlin, DMITRII RACHINSKII, Dallas

Abstract. Systems of operator-differential equations with hysteresis operators can have unstable equilibrium points with an open basin of attraction. Such equilibria can have homoclinic orbits attached to them, and these orbits are robust. In this paper a population dynamics model with hysteretic response of the prey to variations of the predator is introduced. In this model the prey moves between two patches, and the derivative of the Preisach operator is used to describe the hysteretic flow between the patches. A numerical example of a robust homoclinic loop is presented, and a mechanism creating this homoclinic trajectory is discussed.

Keywords: robust homoclinic; orbit Preisach operator; operator-differential equations; predator-prey model

MSC 2010: 47J40, 92D25, 37L15

1. INTRODUCTION

Hysteresis in relationships between various physical variables such as magnetic field and magnetization or mechanical stress and deformation can be modelled by a special class of non-smooth maps called hysteresis operators [19], [7], [28]. For example, constitutive equations of ferromagnetic, elastoplastic, piezoelectric, magnetostrictive and other smart materials have been modelled by the Preisach hysteresis operator and the Prandtl-Ishlinskii hysteresis operator [33], [25], [10], [3], [4]. Macroscopic models where such operator constitutive equations are coupled with differential equations of motion (or some form of Maxwell's equations) [20], [32], [22],

[2], [9], [21], [13], [24], [1], [23] present a class of infinite-dimensional dynamical systems whose dynamics may be substantially different from the dynamics of smooth differential systems [6], [12], [17], [11], [5], [18]. As one example, a coupled system of differential equations

$$(1) \qquad u' = f(u, v), \qquad x' = g(u, v)$$

and an operator equation

$$(2) \qquad x(t) = (\mathcal{P}v)(t)$$

with the Preisach hysteresis operator $\mathcal{P}$ can have an unstable equilibrium which has an open basin of attraction (in the infinite-dimensional phase space of the system). Such equilibria, which have been called partially stable [29], can be compared to a saddle-node singular point of an ordinary differential system. Indeed, they simultaneously attract and repel many trajectories. However, unlike the classical saddle-node point, partially stable equilibria of system (1), (2) are robust.

The rigorous stability analysis presented in [29] for equilibria of equations (1), (2) has been illustrated by prototype examples of a few stable systems including an electronic circuit, a hydrological model, and a predator-prey dynamics model with safe and risky patches. Partially stable equilibria have been found numerically in an epidemiological model of a similar (but different) type [30]. The nature of partial stability suggests that if there is a homoclinic orbit attached to a partially stable equilibrium, then this homoclinic orbit is robust too. This may be interesting, for example because a homoclinic orbit is associated with the so-called excitability phenomenon[1] when the system responds with a pulse to a small perturbation (which is localized in time); such a pulse is a manifestation of a large excursion in the phase space along the homoclinic orbit. Again, robust homoclinic orbits of operator-differential systems contrast with generic homoclinic orbits of smooth differential systems [26] and Filippov's systems [27], [14], as the latter are removable by arbitrarily small perturbations (a homoclinic bifurcation to a saddle or saddle node).

In this paper, we give a numerical evidence that a robust homoclinic orbit exists in a population dynamics model where the prey switches between two modes of behaviour, risky and safe, in response to varying abundance of predator. In the safe state, the prey enjoys lower killing rate by the predator at the price of increased competition rate. The Preisach operator defines how the rate of exchange between

---

[1] The term "excitability" was originally coined in the analysis of the action potential of the axon of the giant Atlantic squid [16]. It is now commonly used to describe any stable dynamical system that exhibits pulses when perturbed above a certain threshold level.

the risky and safe prey populations responds to variations of the predator number. Effectively, it introduces memory in the switching strategy (rule) of the prey.

The homoclinic orbit results from a combination of local dynamics near a partially stable equilibrium and global dynamics which drives those trajectories that leave a small neighbourhood of this equilibrium back to it. The homoclinic trajectory has two parts separated by a point where the predator population achieves its maximum. The trajectory satisfies a different system of ordinary differential equations on each of these two parts. The two ordinary differential systems have the same equilibrium which is unstable for the former system and stable for the latter. Moreover, the switching point belongs to the basin of attraction of the equilibrium of the latter system.

A rigorous proof of existence of a stable homoclinic orbit near the observed numerical solution is beyond the scope of this paper and will be the subject of future work. We note that when stability is analysed, one has to consider not only the perturbations of phase variables (predator and two prey populations), but also the perturbations of the infinite-dimensional memory state of the Preisach operator [31].

The system and a brief description of the Preisach hysteresis operator are presented in the next section, which is followed by the sections presenting numerical results, some related analysis and discussion. The derivation of the model is contained in the Appendix.

2. Excitable behaviour in a predator-prey system

2.1. The model. In this work, we consider a two-patch extension of the model proposed in [15], which has nontrivial dynamical properties such as multiple stable equilibria:

$$(3) \qquad \dot{u}_R = a_R(u_R) - f_R(u_R)g(v) + h_R(t)u_S - h_S(t)u_R,$$

$$(4) \qquad \dot{u}_S = a_S(u_S) - f_S(u_S)g(v) - h_R(t)u_S + h_S(t)u_R,$$

$$(5) \qquad \dot{v} = \sigma(f_R(u_R) + f_S(u_S))g(v) - c(v).$$

Here dot denotes differentiation with respect to time; u_R is the number of prey in the Risky patch; u_S is the number of prey in the Safe patch; v is the number of predator; the terms

$$a_{R/S}(u) = \varrho u - \lambda_{R/S} u^2$$

describe logistic growth of the prey inside the patches with birth rate ϱ and competition rates $\lambda_{R/S}$;

$$f_{R/S}(u) = \frac{\omega_{R/S} u}{\varphi + u}$$

is the Holling type II functional response;

$$g(v) = \frac{v}{1 + \beta v}$$

is the predator interference; σ is the efficiency of conversion of food to growth; and the term

$$c(v) = \gamma v$$

describes death of the predator with the death rate γ. The attack rates for Risky and Safe patches satisfy $\omega_R > \omega_S \geqslant 0$, and we assume that the prey pays a price for choosing the safe patch by higher competition, $\lambda_S > \lambda_R > 0$. A similar two-patch system was considered, e.g., in [8].

There is a flow of prey from the Risky to Safe patch, $h_S(t)u_R$, and in the opposite direction, $h_R(t)u_S$. The simplest choice of the flow rate $h_S(t)$ in one direction is a constant, $h_S(t) = k_{S0}$. In terms of the differentials, $du_S = k_{S0}u_R\, dt$. Another option is to implement a flow in reaction to the change of some function $p(v)$ of the predator number by assuming that $du_S = k_S u_R\, dp(v)$. Combining these two formulas results in

$$h_S(t) = \left(k_{S0} + k_S \frac{dp}{dv}\dot{v}\right)^+,$$

where we ensure that the flow is positive by applying the function $x^+ = \max\{x, 0\}$. Now, equation (5) can be used to substitute for $\dot{v}$. Similarly, $h_R(t) = (k_{R0} - k_R\frac{dp}{dv}\dot{v})^+$.

In this paper, we are interested in the situation when the reaction of prey to variations of the predator population is hysteretic. Namely, we assume that

$$du_S = k_S u_R\, d(\mathcal{P}[\eta_0]v), \quad du_R = -k_R u_S\, d(\mathcal{P}[\eta_0]v),$$

where $\mathcal{P}$ is the Preisach operator with the initial state η_0 [6], and the total flows to the Risky and Safe patches are defined by

$$(6) \qquad h_S(t) = \left(k_{S0} + k_S \frac{d}{dt}(\mathcal{P}[\eta_0]v)(t)\right)^+, \quad h_R(t) = \left(k_{R0} - k_R \frac{d}{dt}(\mathcal{P}[\eta_0]v)(t)\right)^+,$$

respectively. The Preisach operator appears from the assumption that the prey does not respond immediately to a change of the trend in predator dynamics (i.e., the change of the sign of $\dot{v}$). The change of the rate of flows between the patches is delayed until the abundance of predator drops/increases from its extremum value by a certain sufficiently large amount. More detailed derivation of the model is presented in the Appendix.

The Preisach operator is defined by

$$(7) \qquad (\mathcal{P}[\eta_0]v)(t) = \int_0^\infty \int_0^{\alpha_S} \mu(\alpha_R, \alpha_S)(R_{\alpha_R,\alpha_S}[\eta_0(\alpha_R, \alpha_S)]v)(t)\, d\alpha_R\, d\alpha_S,$$

where $v(t)$, $t \geqslant t_0$ is the input; $\mu(\alpha_R, \alpha_S)$ the integrable density function; R_{α_R, α_S} is the non-ideal relay operator with thresholds α_R, α_S satisfying $0 < \alpha_R \leqslant \alpha_S$ (see, for example, [19]); and the function $\eta_0 = \eta_0(\alpha_R, \alpha_S)$ which takes values 0 and 1 represents the initial states of the relays R_{α_R, α_S}. It is convenient to use the standard graphical representation of the states of the relays by points of the domain $0 \leqslant \alpha_R \leqslant \alpha_S$ of the plane (α_R, α_S). It suffices to consider the situation when this domain is divided into two parts by a staircase polyline $\Omega = \Omega(t)$ with the relays in state 1 below (to the left) of this line and in state 0 above (to the right) of this line, see Figure 1 (left). The polyline Ω, which is often referred to as the state of the Preisach operator, can have either a finite or infinite number of horizontal and vertical links, but in the latter case the only accumulation point of the corners is the right end of the polyline; the right end is the point $\alpha_R = \alpha_S = v(t)$ at any moment $t \geqslant t_0$ [19]. A set of simple rules maps the evolution of the input $v(t)$ to the evolution of the polyline $\Omega(t)$ and the output (7) of the Preisach operator; we refer the reader to [19] and Figures 1–2 for the explanation of these rules.
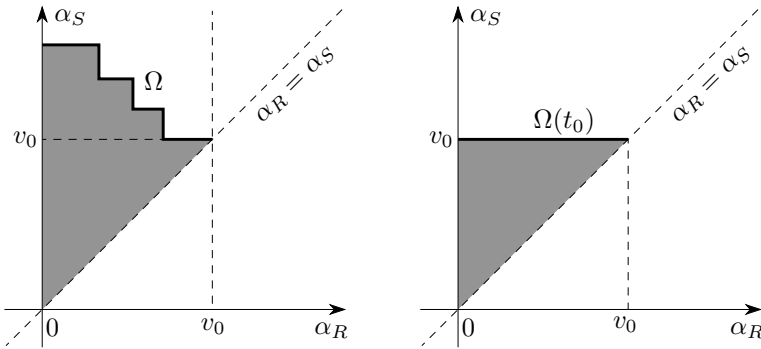

Figure 1. The domain $0 \leqslant \alpha_R \leqslant \alpha_S$ of the plane (α_R, α_S) is divided into two parts by a staircase polyline $\Omega = \Omega(t)$ with the relays in state 1 below (to the left) of this line (grey colour) and in state 0 above (to the right) of this line (white colour). Here $v_0 = v(t_0)$. In the right figure $\Omega(t_0)$ is the horizontal segment $\alpha_S = v(t_0)$, $0 \leqslant \alpha_R \leqslant v(t_0)$.

In equations (3)–(6), the derivative of the output of the Preisach operator is used. For the evaluation of this derivative, the most right link $\Omega_e = \Omega_e(t)$ which is attached to the right end point $\alpha_R = \alpha_S = v(t)$ of the staircase polyline $\Omega(t)$ is of importance, see Figure 3, left (if Ω has infinitely many links, then $\Omega_e = \emptyset$). Denote by (v_m, v), (v, v_M) the end points of the segment Ω_e, where $v_m = v$ if Ω_e is a vertical segment and $v_M = v$ if Ω_e is horizontal. If $v = v(t)$ increases, then the time derivative of the output of the Preisach operator satisfies

$$(8) \qquad \frac{\mathrm{d}(\mathcal{P}[\eta_0]v)}{\mathrm{d}t} = \dot{v} H(v, v_m) \quad \text{with } H(v, v_m) = \int_{v_m}^{v} \mu(\alpha_R, v)\, \mathrm{d}\alpha_R.$$
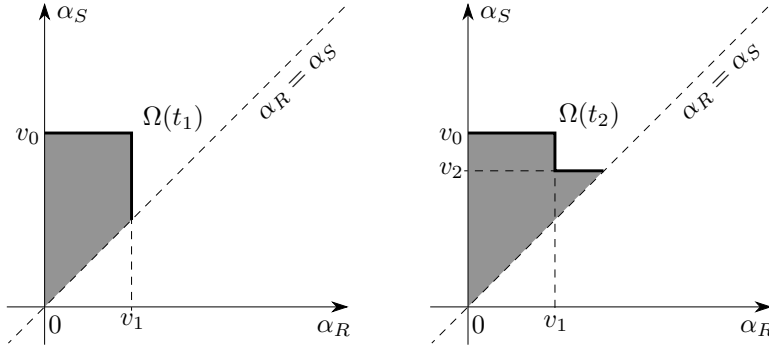
Figure 2. Evolution of the staircase state $\Omega = \Omega(t)$ from the initial state $\Omega(t_0)$ shown in Figure 1 (right) in response to an input $v(t)$ which monotonically decreases on an interval $t \in [t_0, t_1]$. For $t_0 < t \leqslant t_1$ the line Ω consists of two segments. Left panel presents the state at the moment t_1: the vertical link $\alpha_R = v(t_1)$, $v(t_1) \leqslant \alpha_S \leqslant v(t_0)$ connects to the horizontal link, which is part of the segment $\Omega(t_0)$ shown in Figure 1 (right). After the moment t_1, the input $v(t)$ monotonically increases for $t \in [t_1, t_2]$. We assume $v(t_1) < v(t_2) < v(t_0)$. In this case, the state Ω has three links for $t_1 < t \leqslant t_2$ as shown on the right panel for the moment $t = t_2$. The left horizontal link and the vertical link of the line $\Omega(t_2)$ are parts of the staircase $\Omega(t_1)$ presented on the left panel. The extra right horizontal link is $\alpha_S = v(t_2)$, $v(t_1) \leqslant \alpha_R \leqslant v(t_2)$. Here $v_i = v(t_i)$.
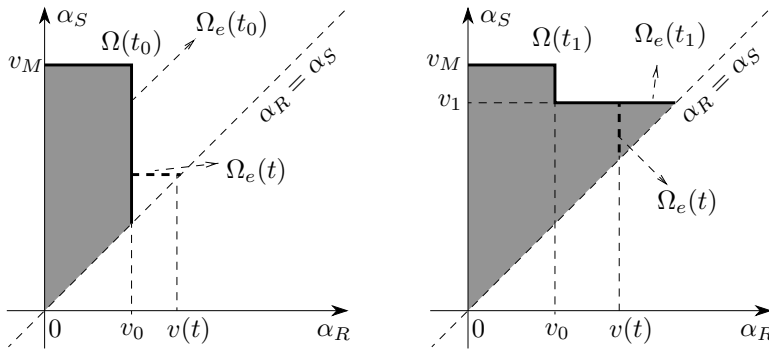

Figure 3. Evolution of the staircase state $\Omega(t)$ for the numerical example of a homoclinic trajectory (see Figures 4, 5); $\Omega_e(t)$ is the lower right segment of this staircase state with the end-point $\alpha_R = \alpha_S = v(t)$ on the bisector. The initial state $\Omega(t_0)$ (solid line on the left panel) consists of a horizontal segment and the vertical segment $\Omega_e(t_0)$. During the time interval $(t_0, t_1]$ when the input $v(t)$ increases, $\Omega(t)$ has three segments, the segment $\Omega_e(t)$ is horizontal (solid dashed line). The right panel shows the state $\Omega(t_1)$ (solid line) at the moment when the input achieves its maximum $v(t_1) = v_1$. After this moment, the input decreases, $\Omega(t)$ consists of four segments, and the segment $\Omega_e(t)$ is vertical (solid dashed line).

If v decreases, then

$$(9) \qquad \frac{\mathrm{d}(\mathcal{P}[\eta_0]v)}{\mathrm{d}t} = \dot{v} V(v, v_M) \quad \text{with} \quad V(v, v_M) = \int_v^{v_M} \mu(v, \alpha_S) \, \mathrm{d}\alpha_S.$$

In the case of increasing v, substituting formula (8) in equations (6), we see that the flows between the patches are equal to

$$(10) \qquad h_S(t) = (k_{S0} + k_S \dot{v} H(v, v_m))^+, \quad h_R(t) = (k_{R0} - k_R \dot{v} H(v, v_m))^+,$$

where $\dot{v}$ can be replaced by the right hand side of equation (5). Similarly, when v decreases,

$$(11) \qquad h_S(t) = (k_{S0} + k_S \dot{v} V(v, v_M))^+, \quad h_R(t) = (k_{R0} - k_R \dot{v} V(v, v_M))^+.$$

Equilibria of system (3)–(7) can be found from the algebraic system, which is obtained by setting the derivatives of all the variables including $(\mathrm{d}/\mathrm{d}t)(\mathcal{P}[\eta_0]v)$ in (3)–(7) to zero. In the next section, we present a numerical example of the homoclinic trajectory (see Figures 4, 5) which is obtained as follows. First, an equilibrium (u_R^*, u_S^*, v^*) of system (3)–(7) is identified, and we choose an initial state $\Omega(t_0)$ of the Preisach operator at the equilibrium with a sufficiently long vertical segment $\Omega_e(t_0)$ (see Figure 3, left). Next, we consider an (arbitrarily) small perturbation of the initial values $(u_R(t_0), u_S(t_0), v(t_0))$ from the equilibrium with $v(t_0) = v^*$ such that $\dot{v}(t_0) > 0$. Hence, initially, $v(t)$ increases, therefore the trajectory of (3)–(7) can be obtained as a solution of the system of ordinary differential equations (3)–(5), (10) with $v_m = v(t_0)$. The choice of parameters ensures that the point (u_R^*, u_S^*, v^*) is an equilibrium of saddle type for this ordinary differential system, hence the solution deviates from the equilibrium. Now, we extend the solution (with the increasing component $v(t)$) to the point where it hits the surface $\dot{v} = 0$ at a moment t_1 (see Figure 3, right). After this moment, $v(t)$ decreases, hence the next segment of the trajectory of system (3)–(7) becomes a solution of ordinary differential system (3)–(5), (11) with $v_M = v(t_1)$. Our choice of parameters ensures that (u_R^*, u_S^*, v^*) is a stable node for this ordinary differential system and that the switching point $(u_R(t_1), u_S(t_1), v(t_1))$ belongs to the basin of attraction of this node. Therefore the trajectory converges back to the equilibrium. In particular, the state $\Omega(t)$ of the Preisach operator converges to its initial state $\Omega(t_0)$ as $t \to \infty$. Summarizing, the homoclinic orbit of system (3)–(7) has two parts, satisfying two different ordinary differential systems which have the same equilibrium. This equilibrium is a saddle for the first system and a node for the other.

2.2. Numerical results. Using a criterion for existence of multiple positive equilibria [15], we set $\varrho = 1.35$, $\varphi = 0.1$, $\beta = 1.2$, $\gamma = 0.5$, $\omega_R = 2$, $\omega_S = 0$ (no predators

in the safe patch), $k_{S0} = 0.01$, $k_{R0} = 0.001$, $\lambda_S = 0.1$, $\lambda_R = 0.01$ to ensure that system (3)–(7) has three positive equilibrium points

(12) $$(u_R^*, u_S^*, v^*) = (0.206995, 13.4915, 0.2904365),$$

(13) $$(u_R^\dagger, u_S^\dagger, v^\dagger) = (0.306704, 13.4923, 0.4235345),$$

(14) $$(u_R^\ddagger, u_S^\ddagger, v^\ddagger) = (133.387, 14.4153, 0.8373).$$

If $k_R = k_S = 0$ (the exchange terms (6) do not have a component with the Preisach operator), then equilibria (12), (13), (14) of the system of ordinary differential equations (3)–(5) have the eigenvalues $(-1.35, 0.084, 0.67)$, $(-1.35, -0.062, 0.89)$, and $(-1.53, -1.33, -0.25)$, respectively. That is, the first and the second equilibria are saddles and the third equilibrium is a stable node.

When the hysteresis terms are present, we give a numerical evidence that equilibrium (12) can become partially stable and can have a homoclinic orbit attached to it. We set $k_R = 0.1 k_S$ and define the density function of the Preisach operator (7) by the formula

$$\mu(\alpha_R, \alpha_S) = \frac{\exp(-900(\alpha_R - 0.2904365)^2)}{0.042}$$

in the triangle $0 \leqslant \alpha_R \leqslant \alpha_S \leqslant 1$, with $\mu = 0$ outside this triangle. The maximum of this Gaussian density distribution corresponds to the equilibrium value v^* of the predator. The integral of μ over the whole half plane $\alpha_S \geqslant \alpha_R$ is normalized to 1.

As the initial state of the Preisach operator we choose the polyline $\Omega(t_0)$ which has two links: a vertical link $\Omega_e(t_0) = \{\alpha_R = v^*, v^* \leqslant \alpha_S \leqslant v_M\}$ and a horizontal link $\{\alpha_S = v_M, 0 \leqslant \alpha_R \leqslant v^*\}$ with $v_M = 1$ (see Figure 3, left). The initial populations are $v(t_0) = v^*, u_R(t_0) \approx u_R^* + 10^{-5}, u_S(t_0) = u_S^*$. For $k_S = 1$, the trajectory of system (3)–(7) starting from these initial values, which are close to equilibrium (12), converges to equilibrium (14) (see Figure 4, dashed line). The component $v(t)$ of this trajectory monotonically increases, hence this trajectory is simultaneously a solution of the ordinary differential system (3)–(5), (10) with $v_m = v(t_0) = v^*$, for which equilibrium (12) is a saddle with eigenvalues

(15) $$(-1.34931, 0.0839766, 0.665618),$$

and equilibrium (14) is a stable node.

Increasing the parameter k_S to the value $k_S = 5.035$, we observe that the trajectory Γ of system (3)–(7) with the same initial values hits the surface $\dot{v} = 0$ at $v(t_1) = 0.3707$. Again, on the interval $[t_0, t_1]$ this trajectory is a solution of the ordinary differential system (3)–(5), (10) (with $v_m = v(t_0) = v^*$), for which the saddle equilibrium (12) has the same eigenvalues (15). However, after the moment t_1

292

the component $v(t)$ of the trajectory Γ of system (3)–(7) decreases and we show numerically that the trajectory Γ is attracted asymptotically towards the same equilibrium (12) near which it started (see Figure 4, solid line). The part of Γ corresponding to $t > t_1$ is a solution of the ordinary differential system (3)–(5), (11) (with $v_M = v(t_1)$), for which the equilibrium (12) is a stable node with the eigenvalues $(-2.66012, -1.34664, -0.0210543)$. Hence, the above results of numerical simulation of system (3)–(7) complemented by the local stability analysis of the associated ordinary differential systems suggest that we have demonstrated a robust homoclinic behaviour in system (3)–(7) with the Preisach hysteresis operator (see Figure 5) by following the plan outlined in the previous subsection.
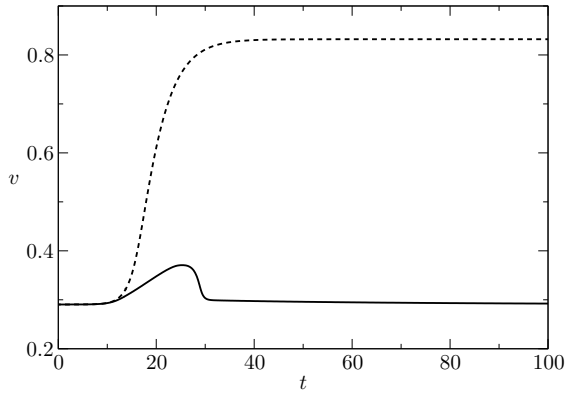

Figure 4. Time series of the predator for two trajectories obtained by a small perturbation of initial data from the equilibrium $(0.206995, 13.4915, 0.2904365)$ (equilibrium (12)) for $k_S = 1$ (dashed line) and $k_S = 5.035$ (solid line).
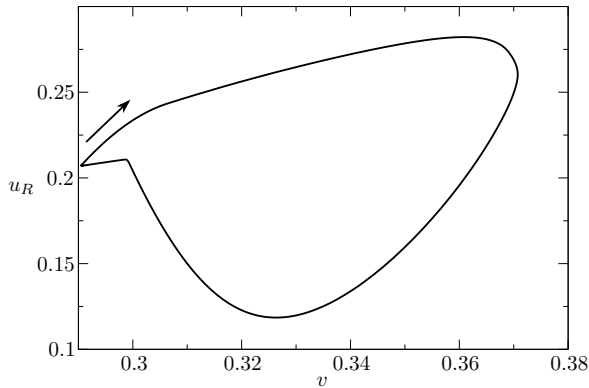

Figure 5. Homoclinic loop for $k_S = 5.035$. The orbit starts from the leftmost point and continues in the direction of the arrow.

Increasing k_S further above the value $k_S = 5.1$, we observe numerically more complicated behaviour of trajectories of system (3)–(7) such as oscillating transients

before convergence to an equilibrium, which for higher values of k_S give rise to a periodic regime (Hopf bifurcation scenario). However, discussion of these dynamics is beyond the scope of the paper.

3. Conclusion

We have proposed a predator-prey model, where the prey can prefer to stay in one of two patches: the Safe patch, where the prey enjoys lower killing rate by the predator at the price of increased competition rate; and the Risky patch. The rate of flow between the patches is assumed to depend on the number of predator; this dependence is described by a hysteresis operator. A mechanism which can produce a homoclinic orbit attached to a partially stable equilibrium of a differential system with hysteresis nonlinearity has been discussed. Using the two-patch predator-prey system as an example, we have demonstrated numerically for the first time a homoclinic orbit that persists for a substantial range of parameter values (a robust homocline).

4. Appendix

We consider a two-layer-type environment, where the top layer corresponds to risky conditions, and the bottom layer corresponds to safe conditions (such as sandy bottom of a natural water reservoir, which can serve as a refuge for some fish species). We assume that the predator species move freely around the whole environment and there is a flow of prey species between Safe and Risky layers. Environment is composed of equally-sized cells such that each cell has both layers (patches) in the same proportion, and the prey moves freely between the cells. Then a change in the number of species in each patch can be represented symbolically in terms of differentials as follows:

Population dynamics	$\mathrm{d}u_R = X_R(u_R, v)\,\mathrm{d}t;$
	$\mathrm{d}u_S = X_S(u_S, v)\,\mathrm{d}t;$
	$\mathrm{d}v = Y(u_R, u_S, v)\,\mathrm{d}t;$
Constant flow from Risky to Safe patch	$\mathrm{d}u_S = -\,\mathrm{d}u_R = k_{S0}u_R\,\mathrm{d}t;$
Constant flow from Safe to Risky patch	$\mathrm{d}u_S = -\,\mathrm{d}u_R = -k_{R0}u_S\,\mathrm{d}t;$
Flow to Safe patch in reaction to v	$\mathrm{d}u_S = -\,\mathrm{d}u_R = k_S u_R\,\mathrm{d}(F_r[\eta_0]v);$
Flow to Risky patch in reaction to v	$\mathrm{d}u_S = -\,\mathrm{d}u_R = k_R u_S\,\mathrm{d}(F_r[\eta_0]v).$

Here

(16)
$$w(t) = (F_r[s_0]v)(t), \quad t \geqslant t_0$$

is the so-called *play* operator [19] of width $2r \geqslant 0$ with the initial state $s_0 \in [-r, r]$, which is defined on the class of all piecewise monotone continuous inputs $v = v(t)$ by the recurrent relationships $w(t_0) = v(t_0) - s_0$ and $w(t) = \varphi_r(v(t), w(t_{i-1}))$, $t \in [t_{i-1}, t_i]$, $i \geqslant 1$, where

$$\varphi_r(v, w) = \max\{v - r, \min\{v + r, w\}\}$$

and $[t_{i-1}, t_i]$ are intervals of monotonicity of the input v. The play operator admits a continuous extension $v(t) \mapsto w(t) = (F_r[s_0]v)(t)$ to the space of continuous functions with the supremum norm; furthermore, the extended play operator has a continuous restriction to the the space of absolutely continuous functions with the $W^{1,1}$-norm [7].

According to the definition of the play operator, the intensity of exchange of prey between the patches responds to the predator abundance $v(t)$ as follows. If v monotonically increases (and $s_0 = r$) or v monotonically decreases (and $s_0 = -r$), then the increments of the rate (16) of flow of prey between the patches are proportional to the increments of the predator abundance, $\mathrm{d}w = \mathrm{d}v$. If $v(t)$ reaches a local maximum at $v(t_1) = v_M$ (or a local minimum at $v(t_2) = v_m$), then there is a window of inactivity such that $\mathrm{d}w/\mathrm{d}t = 0$ while v remains between $v_M - 2r$ and v_M (between v_m and $v_m + 2r$, respectively). After $v(t)$ has reached either end of the inactivity window, the increments of w and v become proportional again, $\mathrm{d}w = \mathrm{d}v$, until v reaches another extremum value and another window of inactivity occurs. In other words, if the trend of predator abundance reverses, the prey hesitates until either the new trend changes the number of predator by $2r$ or until the old trend resumes and the number of predator recovers. Then the prey acts according to the trend of the predator again.

Now, we allow for heterogeneity of the cells of environment by assuming that the width of the inactivity window $2r$ is specific to a cell and has a distribution $\psi(r)$ over all cells. Assuming that the free movement of prey between the cells is much faster than all other processes, we arrive at the averaged formulas for flows between the Safe and Risky patches in response to $v(t)$:

$$\mathrm{d}u_S = -\mathrm{d}u_R = k_S u_R \, \mathrm{d}(P[s_0]v), \quad \mathrm{d}u_S = -\mathrm{d}u_R = k_R u_S \, \mathrm{d}(P[s_0]v),$$

where

(17)
$$(P[s_0]v)(t) = \int_0^\infty \psi(r)(F_r[s_0(r)]v)(t) \, \mathrm{d}s$$

is the Prandtl-Ishlinskii hysteresis operator with the initial state $s_0 = s_0(r)$ [19]. Furthermore, we allow a more general form of the expression for the differentials of the exchange flows by replacing the Prandtl-Ishlinskii operator by the Preisach operator. According to P. Krejčí's formula, the Preisach operator has an equivalent representation

$$(\mathcal{P}[\eta_0]v)(t) = \int_0^\infty \varphi(r, (F_r[s_0(r)]v)(t)) \, \mathrm{d}r.$$

For $\varphi(r, u) = \psi(r)u$, this formula reduces to (17).

Combining the population terms with the hysteretic exchange terms and the constant flows, we obtain the system

$$\dot{u}_R = X_R(u_R, v) + h_R(t)u_S - h_S(t)u_R,$$
$$\dot{u}_S = X_S(u_S, v) - h_R(t)u_S + h_S(t)u_R,$$
$$\dot{v} = Y(u_R, u_S, v)$$

with h_S, h_R defined by formulas (6). System (3)–(7) is obtained by choosing specific population terms $X_{R/S}, Y$ in accordance with the assumptions presented in Section 2.

References

[1] *B. Appelbe, D. Flynn, H. McNamara, P. O'Kane, A. Pimenov, A. Pokrovskii, D. Rachinskii, A. Zhezherun*: Rate-independent hysteresis in terrestrial hydrology. Control Systems Magazine, IEEE *29* (2009), 44–69. DOI 10.1109/MCS.2008.930923.

[2] *B. Appelbe, D. Rachinskii, A. Zhezherun*: Hopf bifurcation in a van der Pol type oscillator with magnetic hysteresis. Physica B: Condensed Matter *403* (2008), 301–304. DOI 10.1016/j.physb.2007.08.034.

[3] *G. Bertotti, I. D. Mayergoyz, C. Serpico*: Nonlinear magnetization dynamics. Switching and relaxation phenomena. The Science of Hysteresis II. Physical Modeling, Micromagnetics, and Magnetization Dynamics (G. Bertotti, I. D. Mayergoyz, eds.). Elsevier, Amsterdam, 2006, pp. 435–565.

[4] *G. Bertotti, I. Mayergoyz*, eds.: The Science of Hysteresis. Elsevier, Amsterdam, 2006.

[5] *M. Brokate, A. Pokrovskii, D. Rachinskii*: Asymptotic stability of continuum sets of periodic solutions to systems with hysteresis. J. Math. Anal. Appl. *319* (2006), 94–109.

[6] *M. Brokate, A. Pokrovskii, D. Rachinskii, O. Rasskazov*: Differential equations with hysteresis via a canonical example. The Science of Hysteresis I. Mathematical Modeling and Applications (G. Bertotti, I. D. Mayergoyz, eds.). Elsevier, Amsterdam, 2006, pp. 125–291.

[7] *M. Brokate, J. Sprekels*: Hysteresis and Phase Transitions. Applied Mathematical Sciences 121, Springer, New York, 1996.

[8] *G. Chiorino, P. Auger, J.-L. Chassé, S. Charles*: Behavioral choices based on patch selection: a model using aggregation methods. Math. Biosci. *157* (1999), 189–216.

[9] *R. Cross, H. McNamara, A. Pokrovskii, D. Rachinskii*: A new paradigm for modelling hysteresis in macroeconomic flows. Physica B: Condensed Matter *403* (2008), 231–236. DOI 10.1016/j.physb.2007.08.017.

[10] *D. Davino, P. Krejčí, C. Visone*: Fully coupled modeling of magneto-mechanical hysteresis through 'thermodynamic' compatibility. Smart Materials and Structures *22* (2013), 14 pages. DOI 10.1088/0964-1726/22/9/095009.

[11] *P. Diamond, N. Kuznetsov, D. Rachinskii*: On the Hopf bifurcation in control systems with a bounded nonlinearity asymptotically homogeneous at infinity. J. Differ. Equations *175* (2001), 1–26.

[12] *P. Diamond, D. Rachinskii, M. Yumagulov*: Stability of large cycles in a nonsmooth problem with Hopf bifurcation at infinity. Nonlinear Anal., Theory Methods Appl. *42* (2000), 1017–1031.

[13] *M. Eleuteri, J. Kopfová, P. Krejčí*: Magnetohydrodynamic flow with hysteresis. SIAM J. Math. Anal. *41* (2009), 435–464.

[14] *M. Guardia, T. M. Seara, M. A. Teixeira*: Generic bifurcations of low codimension of planar Filippov systems. J. Differ. Equations *250* (2011), 1967–2023.

[15] *G. W. Harrison*: Multiple stable equilibria in a predator-prey system. Bull. Math. Biol. *48* (1986), 137–148.

[16] *A. L. Hodgkin, A. F. Huxley*: A quantitative description of membrane current and its application to conduction and excitation in nerve. J. Physiol. *117* (1952), 500–544. DOI 10.1007/BF02459568.

[17] *A. Krasnosel'skii, D. Rachinskii*: On a bifurcation governed by hysteresis nonlinearity. NoDEA, Nonlinear Differ. Equ. Appl. *9* (2002), 93–115.

[18] *A. Krasnosel'skij, D. I. Rachinskij*: On the continua of cycles in systems with hysteresis. Dokl. Math. *63* (2001), 339–344.

[19] *M. A. Krasnosel'skij, A. V. Pokrovskij*: Systems with Hysteresis. Translated from the Russian. Springer, Berlin, 1989.

[20] *P. Krejčí*: Hysteresis, Convexity and Dissipation in Hyperbolic Equations. GAKUTO International Series. Mathematical Sciences and Applications 8, Gakkotosho, Tokyo, 1996.

[21] *P. Krejčí*: On Maxwell equations with the Preisach hysteresis operator: The one-dimensional time-periodic case. Apl. Mat. *34* (1989), 364–374.

[22] *P. Krejčí*: Resonance in Preisach systems. Appl. Math. *45* (2000), 439–468.

[23] *P. Krejčí, J. P. O'Kane, A. Pokrovskii, D. Rachinskii*: Stability results for a soil model with singular hysteretic hydrology. Journal of Physics: Conference Series *268* (2011), 19 pages. DOI 10.1088/1742-6596/268/1/012016.

[24] *P. Krejčí, J. P. O'Kane, A. Pokrovskii, D. Rachinskii*: Properties of solutions to a class of differential models incorporating Preisach hysteresis operator. Physica D. Nonlinear Phenomena *241* (2012), 2010–2028.

[25] *K. Kuhnen, P. Krejčí*: Compensation of complex hysteresis and creep effects in piezoelectrically actuated systems—a new Preisach modeling approach. IEEE Trans. Automat. Control *54* (2009), 537–550.

[26] *Yu. A. Kuznetsov*: Elements of Applied Bifurcation Theory. Applied Mathematical Sciences 112, Springer, New York, 2004.

[27] *Yu. A. Kuznetsov, S. Rinaldi, A. Gragnani*: One-parameter bifurcations in planar Filippov systems. Int. J. Bifurcation Chaos Appl. Sci. Eng. *13* (2003), 2157–2188.

[28] *I. D. Mayergoyz*: Mathematical Models of Hysteresis and Their Applications. Elsevier, Amsterdam, 2003.

[29] *S. McCarthy, D. Rachinskii*: Dynamics of systems with Preisach memory near equilibria. Math. Bohem. *139* (2014), 39–73.

[30] *A. Pimenov, T. C. Kelly, A. Korobeinikov, M. J. O'Callaghan, A. V. Pokrovskii, D. Rachinskii*: Memory effects in population dynamics: spread of infectious disease as a case study. Math. Model. Nat. Phenom. *7* (2012), 204–226.

[31] *A. Pimenov, D. Rachinskii*: Linear stability analysis of systems with Preisach memory. Discrete Contin. Dyn. Syst., Ser. B *11* (2009), 997–1018.

[32] *A. Visintin*: Differential Models of Hysteresis. Applied Mathematical Sciences 111, Springer, Berlin, 1994.

[33] *C. Visone*: Hysteresis modelling and compensation for smart sensors and actuators. Journal of Physics: Conference Series *138* (2008), 23 pages. DOI 10.1088/1742-6596/138/1/012028.

Authors' addresses: *Alexander Pimenov*, Weierstrass Institute, Mohrenstr. 39, 10117 Berlin, Germany, e-mail: `pimenov@wias-berlin.de`; *Dmitrii Rachinskii*, Department of Mathematical Sciences, University of Texas at Dallas, USA, e-mail: `Dmitry.Rachinskiy@utdallas.edu`.